NATIONAL ADVISORY COMMITTEE FOR AERONAUTICS

REPORT 1029

COMPRESSIVE STRENGTH OF FLANGES

By ELBRIDGE Z. STOWELL

1951

For sale by the Superintendent of Documents, U. S. Government Printing Office, Washington 25, D. C. Yearly subscription, $4; foreign, $5.25; single copy price varies according to size . . . . . Price 20 cents

REPORT 1029

COMPRESSIVE STRENGTH OF FLANGES

By ELBRIDGE Z. STOWELL

Langley Aeronautical Laboratory
Langley Field, Va.

National Advisory Committee for Aeronautics

Headquarters, 1724 F Street NW., Washington 25, D. C.

Created by act of Congress approved March 3, 1915, for the supervision and direction of the scientific study of the problems of flight (U. S. Code, title 50, sec. 151). Its membership was increased from 12 to 15 by act approved March 2, 1929, and to 17 by act approved May 25, 1948. The members are appointed by the President, and serve as such without compensation.

REPORT 1029

COMPRESSIVE STRENGTH OF FLANGES [1]

By Elbridge Z. Stowell

SUMMARY

The maximum compressive stress carried by a hinged flange is computed from a deformation theory of plasticity combined with the theory for finite deflections for this structure. The computed stresses agree well with those found experimentally. Empirical observation indicates that the results will also apply fairly well to the more commonly used flanges which are not hinged.

INTRODUCTION

Ordinarily the ability of columns and plates to carry additional load does not entirely cease when they buckle. If the load is increased sufficiently beyond the buckling load, they will ultimately refuse to carry more load, with subsequent permanent distortion. In the case of columns, the maximum load is not far above the buckling load (see reference 1); in the case of plates, there may be a considerable spread between the two loads.

The first essential requirement for the solution of the problem of maximum load is the existence of a finite-deflection theory for the behavior of the structure. Maximum load always occurs at some finite deflection or distortion beyond the buckling load. The problem of the load for a given distortion is thus nonlinear even without the introduction of plasticity. Few such solutions exist for post-buckling behavior of structures even in the elastic region.

The second essential requirement for computation of maximum load is the ability to describe the nonlinear behavior of the structure that results from plasticity of the material. Neither columns nor plates would ever possess a maximum load in compression, if the material of which the structure was made obeyed Hooke's law at all times, although they might be tremendously distorted. In such a structure it would always be possible to add still another increment of load, which would result in still another increment of distortion. The question of a maximum load must therefore be directly linked with the failure of the material to obey Hooke's law—that is, with the plasticity of the material and the nonlinear behavior of the structure which results from that plasticity.

For the calculation of the maximum load carried by a buckled structure, these two essential but difficult requirements must be met. This report treats the maximum compressive strength of a simple plate structure for which the effects of both types of nonlinearity can be found—that is, the compressed flange hinged along one side edge.

The maximum load carried by a long hinged flange is computed as follows: The strain distribution across the flange at any angle of twist is found from knowledge of nonlinearity due to finite deflection. This elastic strain distribution is assumed to persist into the plastic region. This strain distribution is transformed, with the aid of knowledge of nonlinearity due to plasticity, into a stress distribution by means of some appropriate stress-strain relation. The load carried by the flange at the particular twist is then obtained by integrating the stress distribution across the flange. The load is then investigated to see if it has a maximum value as the twist increases; the maximum load should correspond with the experimentally observed maximum load.

Experimental data on the behavior of hinged flanges have been obtained in the Langley Structures Research Division by the methods of reference 2. These data are used in the present report for comparison with theoretical relations.

The theoretical treatment of the behavior of a hinged flange commences in the next section with a discussion of the effects due to finite deflections. Details of the theoretical calculations are presented in two appendixes.

NONLINEAR BEHAVIOR DUE TO FINITE DEFLECTION

Theoretical strain relations.—A flange of length L, width b, and thickness t is shown in figure 1 together with the coordinate system. The flange is hinged along the line $z=0$ and has a free edge along the line $z=b$. Compression is applied longitudinally.

The load is applied uniformly at first. The theory of appendix A shows that, for strains below a certain critical strain ϵ_{cr}, the flange will shorten without twisting. The critical strain ϵ_{cr} at which twisting begins is shown to be

$$\epsilon_{cr}=\frac{(t/b)^2}{2(1+\mu)}+\frac{1}{3}\left(\frac{\pi t}{L}\right)^2 \tag{1}$$

where μ is Poisson's ratio.

As the load is increased beyond that required to start twisting, both the middle-surface strain and the stress distribution across the flange width become nonuniform, larger than the average at the hinge, less than the average at the free edge. The middle-surface strain at any point (x,z) of the flange is shown by the theory of appendix A to be

$$\epsilon_x=\frac{(t/b)^2}{2(1+\mu)}+\frac{m^2}{12}+\frac{5}{24}\frac{k^2m^2}{1+k^2}\left(1-3\frac{z^2}{b^2}\right)\mathrm{sn}^2\left(\frac{4Kx}{L}\right) \tag{2a}$$

[1] Supersedes NACA TN 2020. "Compressive Strength of Flanges" by Elbridge Z. Stowell, 1950.

964418—52

in which k^2 is a parameter lying between 0 and 1 which specifies the amount of twist,

$$K=\int_0^{\pi/2}\frac{d\alpha}{\sqrt{1-k^2\sin^2\alpha}}$$

is the complete elliptic integral of the first kind, and

$$m^2=12\left[\epsilon_{av}-\frac{(t/b)^2}{2(1+\mu)}\right]=K^2(1+k^2)\left(\frac{4t}{L}\right)^2$$

The average middle-surface strain ϵ_{av} in the elastic range is the average stress divided by the elastic modulus E.

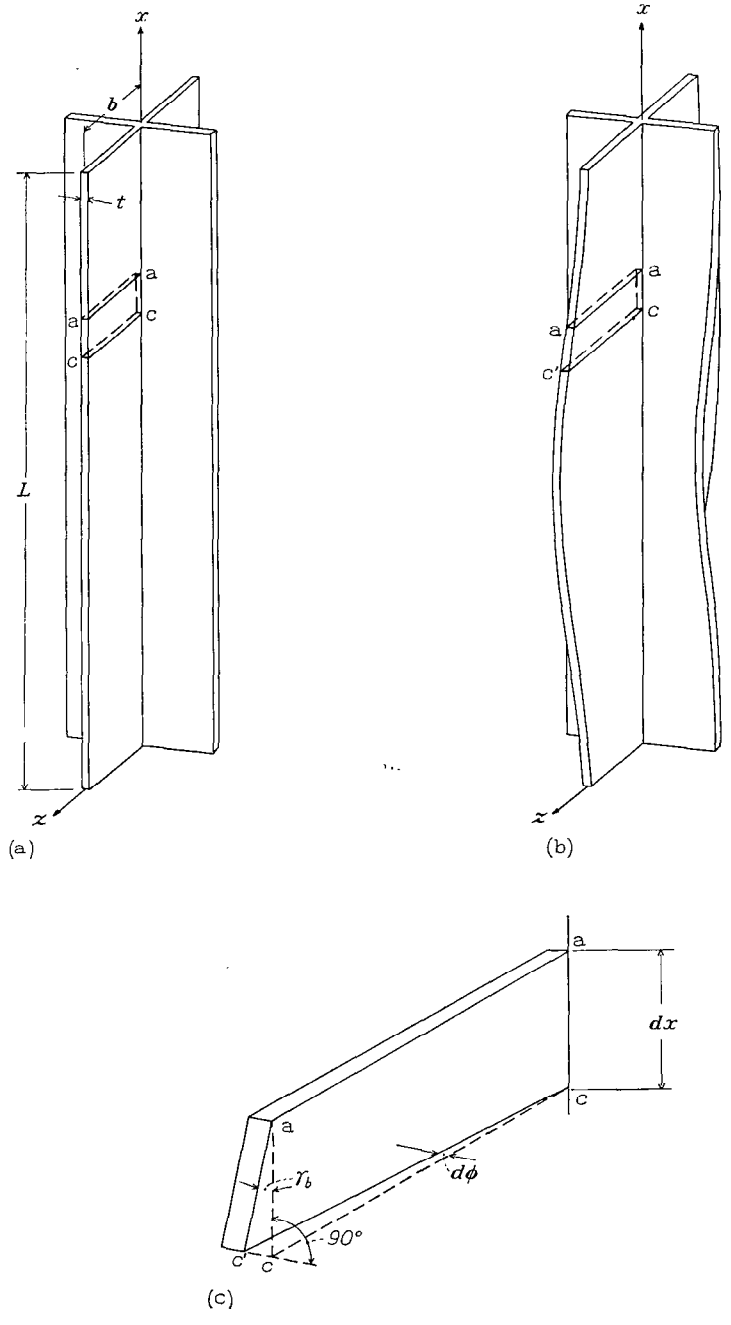

(a) Without distortion. (b) With large distortion.
(c) Enlargement of section aac'c.

FIGURE 1.—Cruciform section, consisting of four identical flanges, before and after buckling. Coordinate system is shown on one flange.

Thus, if a value is assigned to k^2 (a certain amount of twist), both the quantities K and m^2 are determined; the strain at any point (x,z) may then be computed.

Equation (2a) may be simplified as shown in appendix A to the following expression which holds over the essentially straight part of the flange:

$$\epsilon_x=\epsilon_{av}+\frac{5}{4}(\epsilon_{av}-\epsilon_{cr})\left(1-3\frac{z^2}{b^2}\right) \tag{2b}$$

Theory also shows that over most of the flange length (except at the middle and extreme ends) the relation between the middle-surface strain at the hinge ϵ_h, the average middle-surface strain over the width of the flange ϵ_{av}, and the critical strain ϵ_{cr} is

$$\epsilon_{av}=\frac{4}{9}\epsilon_h+\frac{5}{9}\epsilon_{cr} \tag{3}$$

and the rotation ϕ_{max} at the middle of the flange is

$$\phi_{max}=\sqrt{5}\,\frac{t}{b}\cosh^{-1}\frac{1}{\sqrt{1-k^2}} \tag{4a}$$

or approximately

$$\phi_{max}=1.37\,\frac{L}{b}\sqrt{\epsilon_{av}-\epsilon_{cr}}-1.55\,\frac{t}{b} \tag{4b}$$

Relations (1), (2), (3), and (4) are susceptible to experimental check, and the following section describes the results of experiments designed to test these relations.

Experimental check of strain relations.—The hinged flange shown in figure 1 was realized experimentally by the cruciform column shown under test in figure 2. The cruciform column has four identical flanges which, if equally loaded, will twist at the same time without restraint to each other; thus the condition of zero restraint against rotation is fulfilled. The columns were all sufficiently short to cause them to buckle by twisting rather than by Euler bending.

The tests included measurement of the stress-strain curve for the material from which the different groups of specimens were made, determination of the buckling and maximum load for each specimen, a study of the strain distribution across the flanges of two specimens, and a measurement of rotation of each specimen at the middle.

Results of the buckling-load measurements and their connection with the stress-strain curves for the specimens were given in reference 3 and are shown in figure 3 of this report where the buckling stress is plotted against the calculated elastic buckling strain. Because the experimental points follow along the stress-strain curve, the proper reduced modulus for pure twisting in the plastic range is concluded to be the secant modulus, which agrees with the theoretical value of reference 3.

The relation between the computed and experimental middle-surface strain distribution over the width of the flange for one specimen at the quarter height for a number of different loads is shown in figure 4. The highest average stresses exceeded the proportional limit of the material. The measured strains for the four flanges were averaged to give the points shown in the figure. These average strains

were somewhat larger than the ratio of average stress to E at the very highest loads where plasticity reduced the average effective modulus. From the experimentally observed average strain across the flange at each load and the critical strain at which buckling began, the corresponding theoretical strain distributions were computed from equation (2b) and are presented as the curves in figure 4. This calculated strain distribution agrees fairly well with that observed experimentally.

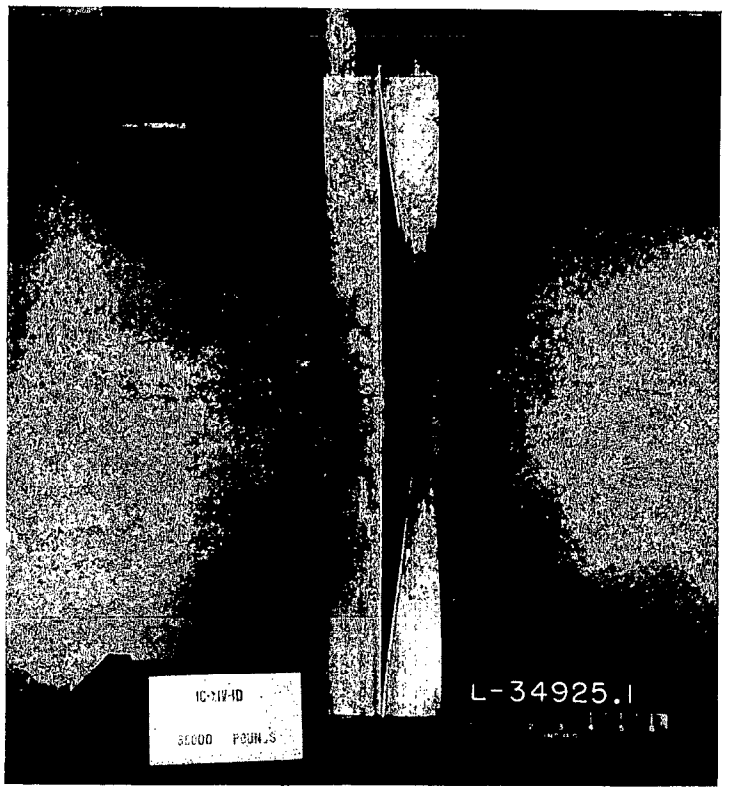

FIGURE 2.—Buckling of a cruciform section in compression.

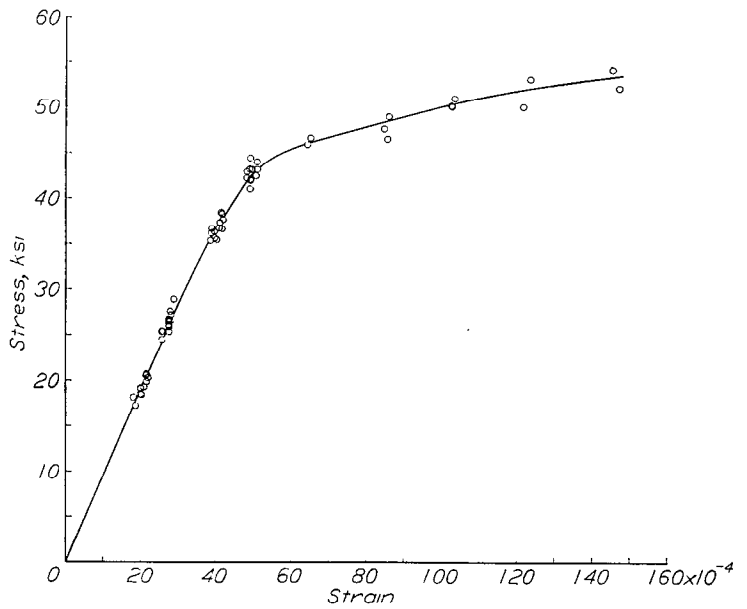

FIGURE 3.—Experimental values of the buckling stress for cruciform-section columns of 24S-T4 extruded aluminum alloy compared with the compressive stress-strain curve for that material.

The relation between average strain, corner strain, and critical strain given by equation (3) was investigated experimentally. From measurement of the strain in two opposite flanges of one buckled specimen, averages were taken to give mean values of ϵ_{av} and ϵ_h. The critical strain ϵ_{cr} was also accurately known. Figure 5 shows the theoretical relation of equation (3) compared with the averaged experimental points. The agreement is good. The strain ϵ_h ceases to be elastic at a value of 0.0025, so that both the curve and the points extend well into the plastic region. The persistence of the agreement between equation (3) and the experimental points up to the highest strains indicates that, even though equation (3) was derived on an elastic basis, it is a good approximation in the plastic region also.

Figure 6 compares the theoretical rotation of three cruciform specimens of widely different lengths with the measured rotations. The ordinate in figure 6 is the shortening δ/L, which is the hinge strain ϵ_h. Rotation was measured by a pointer attached to the flange and moving past a circular scale. Equation (4b) was used to compute the theoretical rotations. The agreement between theory and experiment is good in this case also.

NONLINEAR BEHAVIOR DUE TO PLASTICITY OF THE MATERIAL

The material of the flanges (24S–T aluminum alloy) is defined by the stress-strain curve of figure 3. The figure shows that above 25 ksi the material starts to depart from

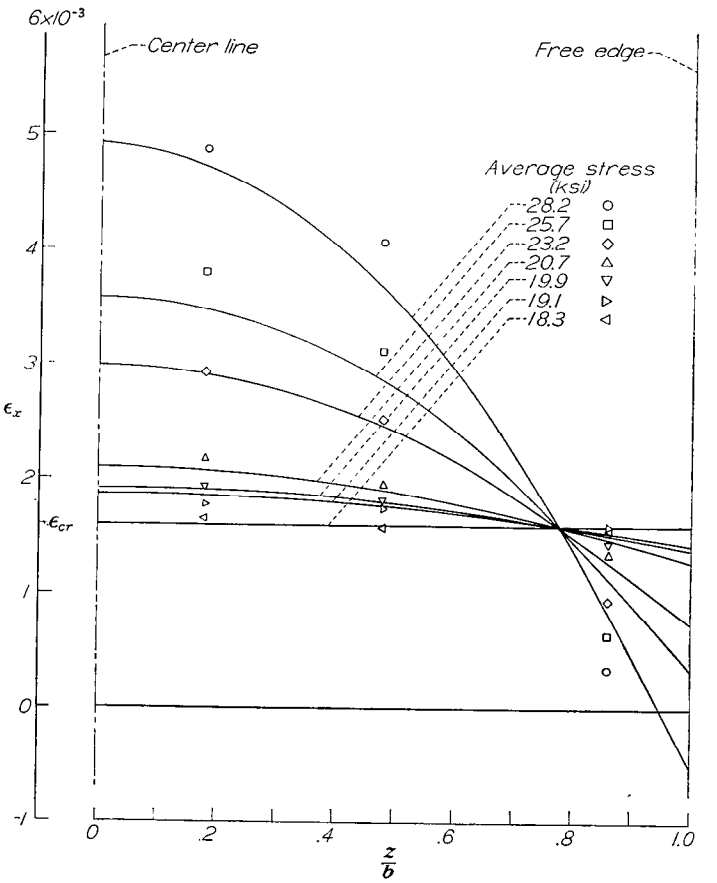

FIGURE 4.—Theoretical middle-surface strain distribution across a hinged flange at the quarter-length station along a cruciform-section column compared with experiment. (Experimental values are average for the four flanges; $\epsilon_{cr}=0.0016$.)

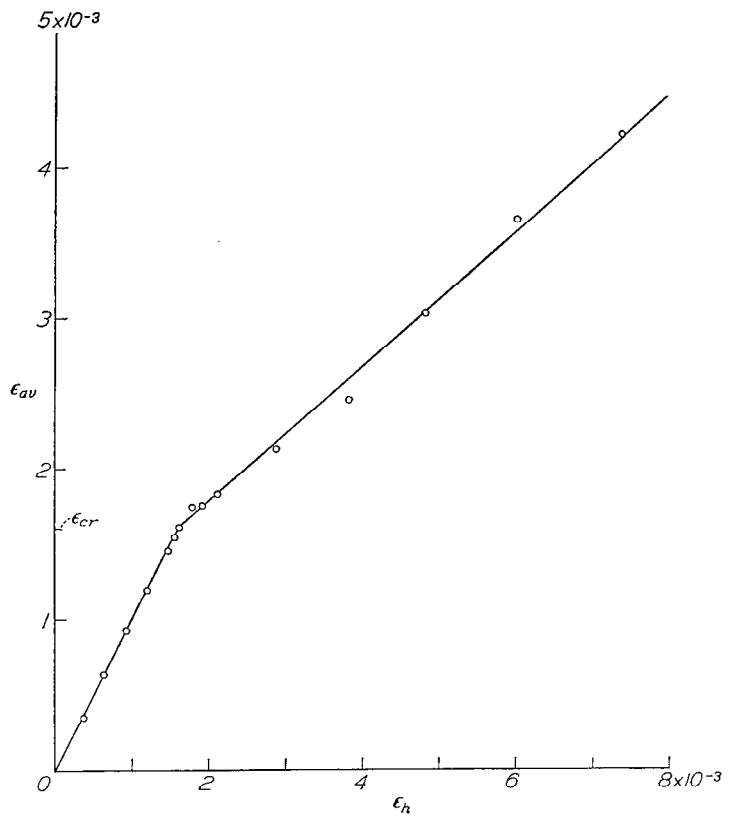

FIGURE 5.—Theoretical middle-surface strain relation between ϵ_{av}, ϵ_h, and ϵ_{cr} for a hinged flange compared with experiment. $\left(\epsilon_{av}=\frac{4}{9}\epsilon_h+\frac{5}{9}\epsilon_{cr} \text{ for } \epsilon_{av}>\epsilon_{cr}.\right)$

purely elastic behavior and becomes partly plastic. As a result of this plasticity, the flanges exhibit nonlinear behavior above about 25 ksi.

The most elementary consequence of the plastic nonlinear behavior is the substitution of E_{sec} for E in the formula for critical stress which, for a hinged flange, is (reference 3)

$$\sigma_{cr}=E_{sec}\epsilon_{cr} \tag{5}$$

Another consequence of the nonlinear behavior due to plasticity is the existence of a maximum load. Experimentally, as the load is increased more and more, the twist of the flange will increase until a value of load is reached at which the flange ceases to carry more load; this value is the maximum load. As was pointed out in the introduction, if the material of the flange obeyed Hooke's law strictly at all times, the rotation of the flange would increase indefinitely with increase in load. The existence of a maximum load is therefore directly attributable to plasticity of the material.

As the structure twists more and more beyond the buckling load, greater and greater shear strains are set up through the thickness of the flange. The shear strains are zero at the middle surface and have opposite signs at the faces. These shear strains will combine with the compressive strain already present to form a strain intensity; at a point where the compressive strain is ϵ_x and the shear strain is γ, the strain intensity is $e_i=\sqrt{\epsilon_x^2+\frac{\gamma^2}{3}}$. (In order not to have to consider variations of γ through the thickness, a mean value of γ^2 is used.) According to the deformation theory of plasticity used herein (reference 3), the value of e_i at any stage of deformation determines the reduced modulus of the material at that stage.

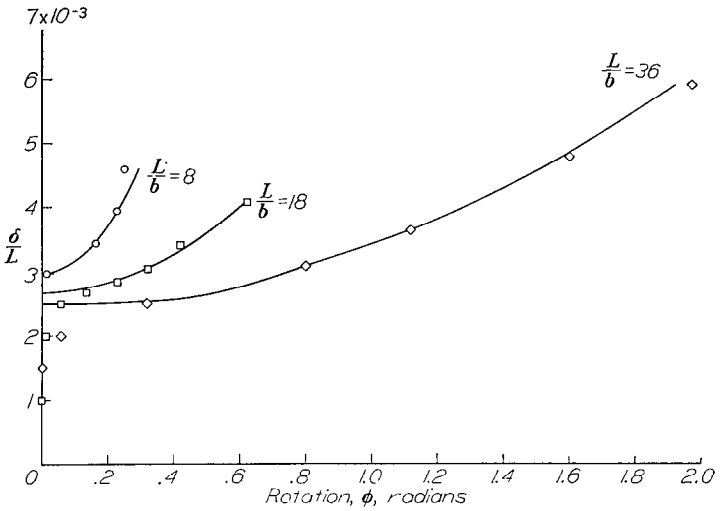

FIGURE 6.—Relation between the shortening δ/L and the rotation ϕ of a hinged flange compared with experiment. $\frac{b}{t}=12$.

Since the maximum load always occurs at a finite rotation of the flange, the two effects of nonlinearity must be combined in order to account for the maximum load. Such a combination is effected in appendix B and the results are given in the following section.

MAXIMUM LOAD OF A FLANGE

It is shown in appendix B how the maximum load on a hinged flange may be computed from the dimensions of the flange and the stress-strain curve for the material.

The middle-surface strain distribution across the flange is given by equation (2a). In addition to these strains which arise directly from the compressive load, there are also shear strains in the flange due to its twist. These shear strains become as large as two-thirds of the compressive strains upon which they are superposed. Although, strictly speaking, the deformation theory of plasticity has only been shown to hold for simple loading (reference 4), its validity is also assumed herein for complex loading. The square of the compressive strains and the mean square of the shear strains were added in the proper manner to give a strain intensity. (The highly localized effects of bending at the middle and ends have been neglected.) From the compressive stress-strain curve for the material the value of the secant modulus E_{sec} was read at this strain intensity. For increasing strain intensities the compressive stress σ at any point across the width of the flange is then simply E_{sec} times the compressive strain at the point. Near the free edge the strain intensity decreases; in such a case, the elastic modulus E is used to compute the corresponding stress reduction. The average stress σ_{av} across the flange is then

$$\sigma_{av}=\frac{1}{b}\int_0^b \sigma\, dz \tag{6}$$

The value of σ_{av} is computed for a number of different twists until a maximum average stress σ_{max} is found.

Figure 7 shows the results plotted in a nondimensional form similar to that employed in reference 2. The parameters used have some theoretical justification and have the effect of making the information given by the plot largely independent of the material. The agreement between the computed curve and the experimental points for cruciform-section columns is satisfactory.

The fact that maximum loads may be computed in this case solely on the basis of deformation theory suggests that the theory is sufficiently accurate when the stress state changes from pure compression to combined compression and shear, for shear strains up to two-thirds of the largest compressive strains.

An interesting side light on this computation is revealed by the values of stress intensity at the supported edge when the load is a maximum. The stress intensity for eight widely different cruciforms is a constant, to about 1 percent, equal to about 47 ksi. (See table 1.) This value is close to the yield stress for the material (46 ksi).

When the flanges are present in actual structures, they are generally connected to other members which offer a certain elastic restraint against rotation along the supported edge. The question arises as to what effect this connection has upon the calculations based on the assumption of a hinge connection. The elastic restraint along the supported edge will have two major effects: The critical strain will be appreciably raised and the effective length L of the buckles will be appreciably shortened. A necessary consequence is that the rotation (which is proportional to L) is reduced and, therefore, is more nearly of the shape of a circular sine along the length of the flange than it would be when a hinge is present along the joint. A third effect is the introduction of a slight curvature across the width of the flange. When the revised critical strain and the revised length are inserted into the formulas of appendix A, which were derived for a flange supported along a hinge, it is found that the rotation and the strain relations may still be accurately predicted for flanges with restraint along the supported edge. Such a result seems to indicate that the small amount of transverse curvature introduced by the restraint does not have an important effect on the formulas.

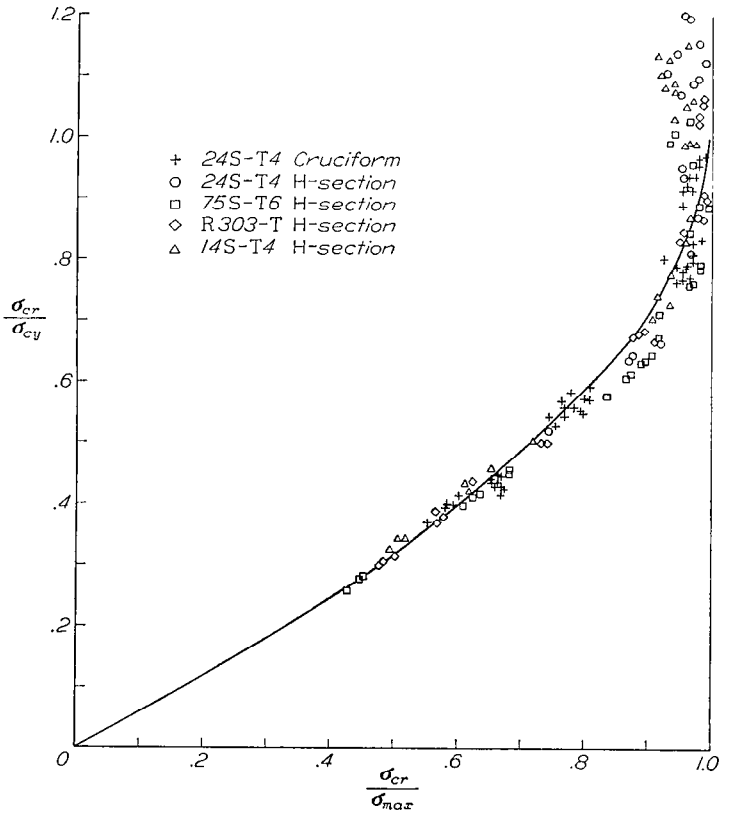

FIGURE 7.—Comparison of theoretical curve for the maximum strength of 24S–T4 aluminum alloy cruciforms with test results. Compressive yield stress $\sigma_{cy}=46$ ksi. (Experimental values for H-sections of various aluminum alloys have been added for comparison with the theoretical curve.)

In view of the fact that the theory of appendix A applies fairly well to flanges with restrained edges, it might be expected that the maximum strength, also, might be given by the same theory. Experiment shows that such is the case; the values of maximum strength for H-sections are included in the experimental points shown in figure 7 and the points intermingle with the cruciform points such that one set cannot be distinguished from the other. The theory of this report may then be said to apply approximately to flanges with elastic restraint along one side edge as well as to flanges without elastic restraint.

CAUSE OF MAXIMUM LOAD

Maximum load occurs when it is no longer possible for the stress, on the average, to grow with increasing strain. The natural tendency for the stress to grow is defeated by the decrease in effective modulus.

In order to illustrate this effect graphically, figures 8(a) and 8(b) have been prepared. These figures illustrate the calculated strain and stress distributions across a hinged flange of 24S–T4 aluminum alloy and of proportions $\frac{b}{t}=14$ and $\frac{L}{b}=12$. These distributions hold over the greater part of the flange where the bending is negligible. Up to the critical strain of 0.002 and the critical stress of 21.5 psi, the distributions are uniform. As the load is increased beyond the critical value, the distributions become more and more nonuniform as a result of twisting of the flange. With increasing load, the strain increases faster at the hinge than at the middle of the flange as shown in figure 8(a). For a time, the corresponding stress also increases faster at the hinge than at the middle of the flange, as shown in figure 8(b). Eventually, however, the strain intensity at the hinge (averaged over the thickness) becomes so large that the modulus is greatly reduced. When that occurs, the stress at the hinge line ceases to grow with increase in strain and even

TABLE 1.—SHOWING CONSTANCY OF STRESS INTENSITY AT HINGE LINE AT MAXIMUM LOAD

Specimen			At failure	
b/t	L/b	σ_{cr} (ksi)	σ_{max} (ksi)	σ_i (ksi)
8	12	45.9	45.7	46.6
9	18	40.6	40.0	45.9
10	4	44.8	44.0	47.5
10	10	37.6	38.0	47.5
11	10	33.4	36.2	47.1
12	4	37.3	39.2	46.6
13	10	25.8	31.5	48.2
14	12	21.7	31.3	48.2

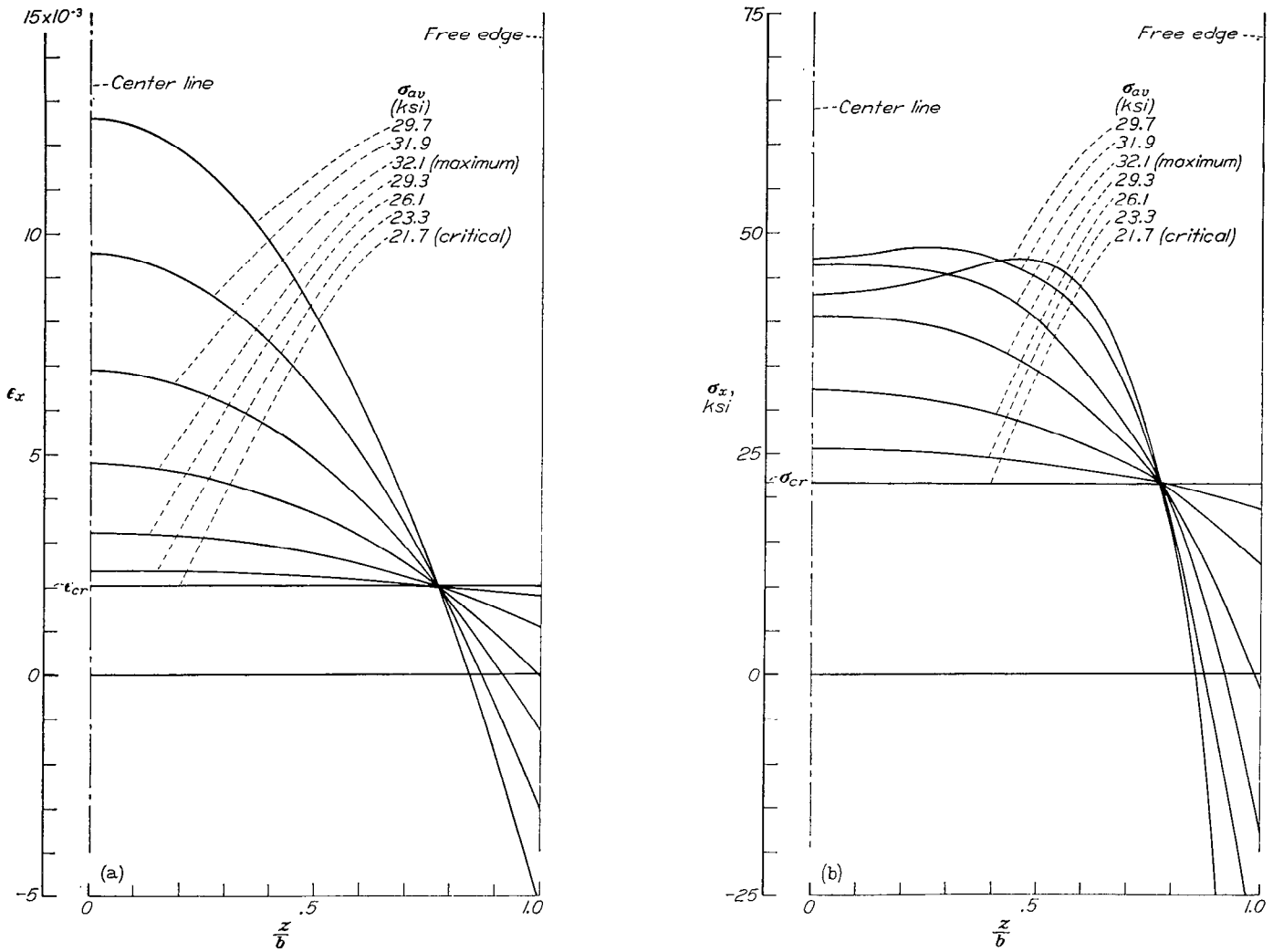

(a) Strain distribution.

(b) Stress distribution.

FIGURE 8.—Theoretical middle-surface strain and stress distribution across a flange at the quarter-length station along a typical cruciform. $\frac{b}{t}=14$; $\frac{L}{b}=12$.

starts to decrease (see fig. 8(b)). The maximum area under the stress curve, and therefore the maximum load, occurs just as the hinge stress starts to recede.

CONCLUSIONS

A theoretical analysis of the compressive strength of flanges, based on a deformation theory of plasticity combined with the theory for finite deflections for this structure, and comparison with experimental data lead to the following conclusions:

1. The maximum load for a flange under compression and hinged along one edge may be accurately computed from the dimensions of the flange and the compressive stress-strain curve for the material.

2. Maximum load occurs when, because of the onset of plasticity, the effective modulus has been reduced to such a low value that it is no longer possible for the average stress to increase with increasing strain. Failure is not a local phenomenon but is an integrated effect over the cross section of the flange.

3. For a wide variety of cruciform sections, the stress intensity (averaged over the thickness) along the hinge line at maximum load is a constant to about 1 percent. This value of stress intensity is very close to the yield stress for the material.

4. The fact that maximum loads may be computed in this case suggests that the deformation theory of plasticity is sufficiently accurate when the stress state changes from compression to combined compression and shear in the case when the shear strains are less than about two-thirds of the compressive strains.

LANGLEY AERONAUTICAL LABORATORY,
NATIONAL ADVISORY COMMITTEE FOR AERONAUTICS,
LANGLEY FIELD, VA., *December 9, 1949.*

APPENDIX A

FINITE DEFLECTION THEORY FOR A HINGED FLANGE UNDER COMPRESSION

ELLIPTIC-FUNCTION SOLUTION

The coordinate system and dimensions of the hinged flange (one-fourth of a cruciform-section column) are shown in figure 1 (a); the form of the distorted shape is shown in figure 1 (b). The fundamental hypothesis of the calculation is that at any section x=Constant there is no curvature of the flange in the direction of z. The correctness of this hypothesis is amply borne out by tests on the flanges while under twist. With this assumption it becomes possible to avoid a formalized plate treatment of the problem.

For infinitesimal rotations, the differential equation of equilibrium for a column under the simultaneous action of a compressive stress σ and torque T has been shown by Wagner (reference 5) to be

$$(GJ-\sigma I_p)\frac{d\phi}{dx}-EC_{BT}\frac{d^3\phi}{dx^3}=T \tag{A1}$$

where

$GJ\frac{d\phi}{dx}$ St. Venant component of internal resisting torque

$\sigma I_p\frac{d\phi}{dx}$ component of internal torque due to application of compressive force. (This component is not a resisting torque but aids the applied torque T in twisting the column; its sign is therefore negative.)

$-EC_{BT}\frac{d^3\phi}{dx^3}$ component of internal resisting torque due to bending of column as it twists

For the case in which the applied torque T is zero, such as for a compressed hinged flange, equation (A1) becomes

$$(GJ-\sigma I_p)\frac{d\phi}{dx}-EC_{BT}\frac{d^3\phi}{dx^3}=0 \tag{A2}$$

As previously mentioned, equations (A1) and (A2) are limited to infinitesimal rotations and thus cannot be used to determine the behavior of a column above the buckling load where rotations may become large.

In order to investigate the behavior of a compressed hinged flange above buckling, a theory which permits the calculation of the large deformations which may occur after buckling must be employed. The differential equation (A2) must therefore be amended to include the effects which appear at finite values of the rotation ϕ.

DERIVATION OF THE BASIC DIFFERENTIAL EQUATION FOR FINITE ROTATIONS

The effects of finite rotation involve the changes in the middle-surface strain that occur after buckling. As the plate twists, the longitudinal fibers will be inclined at a small angle to the hinge line as shown in figure 1 (b). As a result, the longitudinal fibers are stretched in varying amounts and the horizontal components of the forces along the fibers produce a torque which resists twisting of the plate. The resisting torque increases very rapidly with twisting of the plate, which thus becomes progressively stiffer. The rapid increase of stiffness with rotation provides the required mechanism for maintaining the rotation at a finite value.

Stretching of middle-surface fibers after buckling.—A short section of the plate as shown in figure 1 (c) will have the length ac before the plate buckles. After buckling, the length ac′ will be greater than ac because ac′ is inclined at an angle γ_b with the hinge line. (See fig. 1 (c).) Thus the strain at the free edge ϵ_b due to stretching for small values of γ_b is

$$-\epsilon_b=\frac{ac'-ac}{ac}=\sec\gamma_b-1\approx\frac{\gamma_b^2}{2} \tag{A3}$$

(The strain ϵ_b is positive when compressive.)

If the line aa (fig. 1 (c)) has been rotated an angle ϕ from its original position, the free-edge fiber at c moves a distance $b(\phi+d\phi)$. The angle of inclination of the free-edge fiber is thus

$$\gamma_b=\frac{b(\phi+d\phi)-b\phi}{dx}=b\frac{d\phi}{dx} \tag{A4}$$

If the point c is not at the free edge but at some interior position a distance z from the hinge line, it can similarly be shown that

$$-\epsilon_z=\frac{\gamma_z^2}{2} \tag{A5}$$

$$\gamma_z=z\frac{d\phi}{dx} \tag{A6}$$

From equations (A5) and (A6), the strain ϵ_z resulting from the stretching action can be given as

$$\epsilon_z=-\frac{z^2}{2}\left(\frac{d\phi}{dx}\right)^2 \tag{A7}$$

Equation (A7) gives the difference between the hinge-line strain and the strain at any fiber due to the stretching action, for a given position along the width of the flange. It is this

difference which causes the middle-surface strain distribution after buckling to differ from the uniform strain distribution at the instant of buckling and which will now be considered.

Middle-surface strain distribution after buckling.—A compressive load P applied to the hinged flange will cause the ends to approach each other by a distance δ. The unit shortening e is δ/L. Equilibrium of the internal compressive forces with the applied force P requires that

$$P=tE\int_0^b (e+\epsilon_z)\cos\gamma_z\,dz \tag{A8}$$

The angle γ_z is usually so small that $\cos\gamma_z$ may be taken as unity. Then, substituting the expression for ϵ_z from equation (A7) into equation (A8) yields

$$P=tE\int_0^b\left[e-\frac{z^2}{2}\left(\frac{d\phi}{dx}\right)^2\right]dz=EA\left[e-\frac{b^2}{6}\left(\frac{d\phi}{dx}\right)^2\right] \tag{A9}$$

The unit shortening e is therefore

$$e=\frac{P}{AE}+\frac{b^2}{6}\left(\frac{d\phi}{dx}\right)^2 \tag{A10}$$

The ratio P/AE is the average strain over the cross section. If P/AE is denoted by ϵ_{av}, equation (A10) becomes

$$e=\epsilon_{av}+\frac{\gamma_b^2}{6} \tag{A11}$$

The longitudinal middle-surface strain ϵ_x at any fiber z in the cross section is therefore

$$\epsilon_x=e+\epsilon_z=\epsilon_{av}+\frac{\gamma_b^2}{6}-\frac{z^2}{2}\left(\frac{d\phi}{dx}\right)^2 \tag{A12}$$

Moment due to axial stress after buckling.—The longitudinal strain ϵ_x does not have the direction of the hinge line but of the slightly inclined longitudinal fibers (the angle γ_z, equation (A6)). Consequently, $E\epsilon_x$ has components perpendicular to the hinge line which create the moment ΔM resulting from the applied compressive force.

The component of $E\epsilon_x$ perpendicular to the hinge line at any fiber z is $E\epsilon_x\sin\gamma_z$ and for small angles is approximately equal to $E\epsilon_x z\frac{d\phi}{dx}$. As this component has a lever arm z, the internal resisting moment ΔM is

$$\Delta M=-Et\int_0^b\left(\epsilon_x z\frac{d\phi}{dx}\right)z\,dz \tag{A13}$$

Substituting the expression for ϵ_x from equation (A12) into equation (A13) results in the following relationship:

$$\Delta M=-\sigma I_p\frac{d\phi}{dx}+\frac{2}{15}Eb^2I_p\left(\frac{d\phi}{dx}\right)^3 \tag{A14}$$

The term $\sigma I_p\frac{d\phi}{dx}$ is the same term that appears in equation (A2). The last term of equation (A14) is the required additional term which takes into account the stretching actions, which occur for finite rotations of the flange, and permits the computation of the rotation ϕ.

Basic differential equation of torque for a compressed hinged flange which includes the effects of finite rotation.—The complete differential equation of torque which replaces equation (A2) and includes the last term of equation (A14) is

$$(GJ-\sigma I_p)\frac{d\phi}{dx}-EC_{BT}\frac{d^3\phi}{dx^3}+\frac{2}{15}Eb^2I_p\left(\frac{d\phi}{dx}\right)^3=0 \tag{A15}$$

The constants of equation (A15) are

$$\left.\begin{aligned} J&=\frac{bt^3}{3}\\ I_p&=\frac{b^3t}{3}\\ C_{BT}&=\frac{b^3t^3}{36}\\ G&=\frac{E}{2(1+\mu)}\end{aligned}\right\} \tag{A16}$$

Substituting equations (A16) into (A15) yields

$$\frac{d^3\phi}{dx^3}+\frac{12}{t^2}\left[\epsilon_{av}-\frac{(t/b)^2}{2(1+\mu)}\right]\frac{d\phi}{dx}-\frac{8}{5}\left(\frac{b}{t}\right)^2\left(\frac{d\phi}{dx}\right)^3=0 \tag{A17}$$

A further simplification is effected by the use of

$$\left.\begin{aligned} \gamma_b&=b\frac{d\phi}{dx}\\ \xi&=\frac{x}{t}\\ m^2&=12\left[\epsilon_{av}-\frac{(t/b)^2}{2(1+\mu)}\right]\end{aligned}\right\} \tag{A18}$$

The substitution of relations (A18) into equation (A17) gives the basic differential equation for a compressed hinged flange

$$\frac{d^2\gamma_b}{d\xi^2}+m^2\gamma_b-\frac{8}{5}\gamma_b^3=0 \tag{A19}$$

SOLUTION OF THE BASIC DIFFERENTIAL EQUATION FOR FINITE ROTATION

The basic differential equation (A19) has the solution

$$\xi+\xi_0=\pm\int\frac{d\gamma_b}{\sqrt{c^2-m^2\gamma_b^2+\frac{4}{5}\gamma_b^4}} \tag{A20}$$

where c and ξ_0 are constants of integration. (The sign of

the radical must be chosen so as to keep $d\xi$ positive.) With the condition that $\gamma=0$ for $\xi=0$ $\left(\frac{d\phi}{dx}\text{ equals zero at the ends}\right)$ and the substitutions

$$\left.\begin{aligned} g^2&=\frac{m^2}{2}+\sqrt{\frac{m^4}{4}-\frac{4}{5}c^2}\\ h^2&=\frac{m^2}{2}-\sqrt{\frac{m^4}{4}-\frac{4}{5}c^2}\end{aligned}\right\} \tag{A21}$$

equation (A20) may be written

$$\xi=\int_0^{\gamma_b}\frac{d(\gamma_b/c)}{\sqrt{[1-g^2(\gamma_b/c)^2]\,[1-h^2(\gamma_b/c)^2]}} \tag{A22}$$

With new variables Ψ and k defined by

$$\left.\begin{aligned} \frac{1}{g}\sin\Psi&=\frac{\gamma_b}{c}\\ k&=\frac{h}{g}\end{aligned}\right\} \tag{A23}$$

equation (A22) is transformed into

$$\xi=\frac{1}{g}\int_0^{\Psi}\frac{d\Psi}{\sqrt{1-k^2\sin^2\Psi}} \tag{A24}$$

In order to determine the constant c, use is made of the condition that $\gamma_b=0$ for $\xi=\frac{L}{2t}$ or $x=\frac{L}{2}$. The upper limit for equation (A24) corresponding to $x=\frac{L}{2}$ must then be $\Psi=\pi$ in order to satisfy the first of equations (A23):

$$\frac{L}{2t}=\frac{1}{g}\int_0^{\pi}\frac{d\Psi}{\sqrt{1-k^2\sin^2\Psi}}$$

or

$$g=\frac{4t}{L}\int_0^{\pi/2}\frac{d\Psi}{\sqrt{1-k^2\sin^2\Psi}} \tag{A25}$$

In elliptic-function notation,

$$\left.\begin{aligned} \int_0^{\pi/2}\frac{d\alpha}{\sqrt{1-k^2\sin^2\alpha}}&=K(k)\\ \int_0^{\Psi}\frac{d\alpha}{\sqrt{1-k^2\sin^2\alpha}}&=\mathrm{sn}^{-1}(\sin\Psi)=\mathrm{sn}^{-1}\left(\frac{g\gamma_b}{c}\right)\end{aligned}\right\} \tag{A26}$$

Equation (A25) therefore may be written

$$g=\frac{4Kt}{L} \tag{A27}$$

and equation (A24) becomes

$$\frac{4Kx}{L}=\int_0^{\Psi}\frac{d\alpha}{\sqrt{1-k^2\sin^2\alpha}}=\mathrm{sn}^{-1}\left(\frac{g\gamma_b}{c}\right)$$

so that taking the elliptic sine of both sides gives

$$\gamma_b=\frac{c}{g}\,\mathrm{sn}\left(\frac{4Kx}{L}\right) \tag{A28}$$

The coefficient c/g is readily found from the definitions of g and h in equations (A21). From the first of these equations

$$h=\sqrt{m^2-g^2}=\sqrt{12}\sqrt{\epsilon_{av}-\frac{(t/b)^2}{2(1+\mu)}-\frac{g^2}{12}}$$

and from the second

$$\frac{c}{g}=\frac{\sqrt{5}}{2}\,h=\sqrt{15}\sqrt{\epsilon_{av}-\frac{(t/b)^2}{2(1+\mu)}-\frac{g^2}{12}}$$

Making use of equation (A27) leads to the general solution

$$\gamma_b=\sqrt{15}\sqrt{\epsilon_{av}-\frac{(t/b)^2}{2(1+\mu)}-\frac{1}{12}\left(\frac{4Kt}{L}\right)^2}\,\mathrm{sn}\left(\frac{4Kx}{L}\right) \tag{A29}$$

Another form of the solution which is sometimes convenient may be obtained by using a different expression for h: Since addition of equations (A21) gives

$$m^2=g^2+h^2=g^2(1+k^2)=\left(\frac{4Kt}{L}\right)^2(1+k^2) \tag{A30}$$

it follows that

$$g=\frac{m}{\sqrt{1+k^2}}$$

and that

$$h=kg=\frac{km}{\sqrt{1+k^2}}$$

Hence,

$$\gamma_b=\frac{\sqrt{5}}{2}\,h\,\mathrm{sn}\left(\frac{4Kx}{L}\right)=\frac{\sqrt{5}}{2}\,\frac{km}{\sqrt{1+k^2}}\,\mathrm{sn}\left(\frac{4Kx}{L}\right) \tag{A31}$$

With either equation (A29) or equation (A31) now available as an accurate expression for the fiber slope γ_b, it is possible, besides checking the known formula for the critical compressive stress, to write formulas also for the rotation at any station along the flange, for the middle-surface strain distribution along and across the flange, for the relation between hinge-line, average, and critical strains, and for the fractional shortening. The formulas will now be given in that order.

Check of critical compressive stress.—In order to show that equations (A29) or (A31) give the correct buckling stress at the start of the rotation ($\gamma_b=0$), the behavior of the elliptic function is considered as the rotation approaches zero.

The preceding section showed that the angle γ_b is proportional to h, and therefore to k. As k approaches zero, K approaches $\pi/2$, and the elliptic sine approaches the circular sine. Hence for loads only slightly above the critical, from equation (A29),

$$\gamma_b=\sqrt{15}\sqrt{\epsilon_{av}-\frac{(t/b)^2}{2(1+\mu)}-\frac{1}{12}\left(\frac{2\pi t}{L}\right)^2}\sin\frac{2\pi x}{L}$$

At the critical load, $\gamma_b=0$, and for loaded edges clamped,

$$(\epsilon_{av})_{\gamma_b=0}=\epsilon_{cr}=\frac{(t/b)^2}{2(1+\mu)}+\frac{1}{12}\left(\frac{2\pi t}{L}\right)^2 \tag{A32}$$

This is the expression given as equation (1) in the body of the report. The critical compressive stress σ_{cr} is obtained by multiplying both sides of equation (A32) by the effective modulus in compression E_{sec}. Then

$$\sigma_{cr}=E_{sec}\epsilon_{cr}=E_{sec}\left[\frac{(t/b)^2}{2(1+\mu)}+\frac{1}{12}\left(\frac{2\pi t}{L}\right)^2\right] \tag{A33}$$

This is the expression given as equation (5) in the body of the report.

Rotation of any station along the flange.—By symmetry, the rotation of any station a distance x from either end is given by

$$\phi=\frac{L}{b}\int\gamma_b\,d\left(\frac{x}{L}\right) \tag{A34}$$

and so is obtained by a simple integration of the fiber angle distribution along the length of the flange, subject to the condition that the rotation is zero at both ends of the flange.

If an analytical expression for ϕ is desired, either equation (A29) or its alternate (A31) may be integrated. Integration of equation (A31) gives

$$\phi=\frac{\sqrt{5}}{2}\frac{km}{\sqrt{1+k^2}}\frac{L}{4bK}\int_0^{4Kx/L}\mathrm{sn}\left(\frac{4Kx}{L}\right)d\left(\frac{4Kx}{L}\right)$$

$$=\frac{\sqrt{5}}{2}\frac{m}{\sqrt{1+k^2}}\frac{L}{4bK}\left[\cosh^{-1}\frac{1}{\sqrt{1-k^2}}-\cosh^{-1}\frac{\sqrt{1-k^2\mathrm{sn}^2(4Kx/L)}}{\sqrt{1-k^2}}\right] \tag{A35}$$

Since

$$m=g\sqrt{1+k^2}=\frac{4Kt}{L}\sqrt{1+k^2}$$

the general integral becomes

$$\phi=\frac{\sqrt{5}}{2}\frac{t}{b}\left[\cosh^{-1}\frac{1}{\sqrt{1-k^2}}-\cosh^{-1}\frac{\sqrt{1-k^2\mathrm{sn}^2(4Kx/L)}}{\sqrt{1-k^2}}\right] \qquad \left(\frac{1}{4}\geqq\frac{x}{L}\geqq 0;\ 1\geqq\frac{x}{L}\geqq\frac{3}{4}\right)$$

$$\phi=\frac{\sqrt{5}}{2}\frac{t}{b}\left[\cosh^{-1}\frac{1}{\sqrt{1-k^2}}+\cosh^{-1}\frac{\sqrt{1-k^2\mathrm{sn}^2(4Kx/L)}}{\sqrt{1-k^2}}\right] \qquad \left(\frac{3}{4}\geqq\frac{x}{L}\geqq\frac{1}{4}\right)$$

$$\phi=\frac{\sqrt{5}}{2}\frac{t}{b}\cosh^{-1}\frac{1}{\sqrt{1-k^2}} \qquad \left(\frac{x}{L}=\frac{1}{4}\text{ or }\frac{x}{L}=\frac{3}{4}\right)$$

$$\phi_{max}=\sqrt{5}\frac{t}{b}\cosh^{-1}\frac{1}{\sqrt{1-k^2}} \qquad \left(\frac{x}{L}=\frac{1}{2}\right)$$

Variation of middle-surface strain over length and width of flange.—The middle-surface strain ϵ_x at any distance z from the hinge line was given in equation (A12) as

$$\epsilon_x=\epsilon_{av}+\frac{\gamma_b^2}{6}\left(1-3\frac{z^2}{b^2}\right)$$

The slope of the free-edge fiber γ_b may now be inserted in this expression from either equation (A29) or equation (A31). Thus

$$\epsilon_x=\epsilon_{av}+\frac{5}{2}\left[\epsilon_{av}-\frac{(t/b)^2}{2(1+\mu)}-\frac{1}{12}\left(\frac{4Kt}{L}\right)^2\right]\left(1-3\frac{z^2}{b^2}\right)\mathrm{sn}^2\left(\frac{4Kx}{L}\right) \tag{A36a}$$

or

$$\epsilon_x=\epsilon_{av}+\frac{5}{24}\frac{k^2m^2}{1+k^2}\left(1-3\frac{z^2}{b^2}\right)\mathrm{sn}^2\left(\frac{4Kx}{L}\right) \tag{A36b}$$

or

$$\epsilon_x=\frac{\left(\frac{t}{b}\right)^2}{2(1+\mu)}+\frac{m^2}{12}+\frac{5}{24}\frac{k^2m^2}{1+k^2}\left(1-3\frac{z^2}{b^2}\right)\mathrm{sn}^2\left(\frac{4Kx}{L}\right) \tag{A36c}$$

Relationships between hinge-line, average, and critical strains.—Along the hinge line $z=0$, and equations (A36) give

$$(\epsilon_x)_{z=0}=\epsilon_{av}+\frac{5}{2}\left[\epsilon_{av}-\frac{(t/b)^2}{2(1+\mu)}-\frac{1}{12}\left(\frac{4Kt}{L}\right)^2\right]\mathrm{sn}^2\left(\frac{4Kx}{L}\right)$$

or

$$(\epsilon_x)_{z=0}=\epsilon_{av}+\frac{5}{24}\frac{k^2m^2}{1+k^2}\,\mathrm{sn}^2\left(\frac{4Kx}{L}\right)$$

Along the hinge line at $x=\frac{L}{4}$ and $x=\frac{3L}{4}$,

$$(\epsilon_x)_{z=0}=\frac{7}{2}\,\epsilon_{av}-\frac{5}{2}\left[\frac{(t/b)^2}{2(1+\mu)}+\frac{1}{12}\left(\frac{4Kt}{L}\right)^2\right] \qquad \text{(A37a)}$$

or

$$(\epsilon_x)_{z=0}=\epsilon_{av}+\frac{5}{24}\frac{k^2m^2}{1+k^2} \qquad \text{(A37b)}$$

Along the hinge line at $x=0$, $x=\frac{L}{2}$, and $x=L$,

$$(\epsilon_x)_{z=0}=\epsilon_{av}$$

Thus at the ends and at the middle the strain is uniformly distributed across the width of the hinged flanges.

Fractional shortening.—The fractional shortening of the flange δ/L (1/4 of its length is considered for convenience) is

$$\begin{aligned}
e&=\frac{\delta}{L}\\
&=\frac{4}{L}\int_0^{L/4}(\epsilon_x)_{z=0}\,dx\\
&=\frac{1}{K}\int_0^{K}(\epsilon_x)_{z=0}\,d\left(\frac{4Kx}{L}\right)\\
&=\epsilon_{av}+\frac{5}{24}\frac{k^2m^2}{1+k^2}\frac{1}{K}\int_0^{K}\mathrm{sn}^2\left(\frac{4Kx}{L}\right)d\left(\frac{4Kx}{L}\right)\\
&=\epsilon_{av}+\frac{5}{24}\frac{m^2}{1+k^2}\left(1-\frac{E}{K}\right)
\end{aligned}$$

where $E=\int_0^{\pi/2}\sqrt{1-k^2\sin^2\alpha}\,d\alpha$. From equation (A30) $m=\frac{4Kt}{L}\sqrt{1+k^2}$, and by use of this value of m,

$$e=\frac{\delta}{L}=\epsilon_{av}+\frac{10}{3}\left(\frac{t}{L}\right)^2K(K-E) \qquad \text{(A38)}$$

APPROXIMATE RELATIONSHIPS FOR POSTBUCKLING BEHAVIOR

The preceding relationships for the behavior of a hinged flange when compressed beyond the buckling load may be greatly simplified if the flange is long enough so that bending is negligible compared with the twist. Under such conditions the term $EC_{BT}\frac{d^3\phi}{dx^3}$ in the differential equation (A15) may be neglected. The basic differential equation (A19) then reduces to a simple algebraic equation

$$m^2\gamma_b-\frac{8}{5}\gamma_b^3=0$$

The fiber angle γ_b.—Solutions of the preceding equation are

$$\gamma_b=0$$

and

$$\gamma_b=\pm\sqrt{\frac{5}{8}}\,m=\pm\sqrt{\frac{15}{2}}\sqrt{\epsilon_{av}-\epsilon_{cr}} \qquad \text{(A39)}$$

in which $\epsilon_{cr}=\frac{(t/b)^2}{2(1+\mu)}$, the term in length now being omitted. The same quantities which were computed under "Elliptic Function Solution" may now be expressed once more in terms of the approximate solution for γ_b.

Rotation of flange.—The approximate rotation will be the integral of the approximate value of γ_b, or

$$\phi=\sqrt{\frac{15}{2}}\sqrt{\epsilon_{av}-\epsilon_{cr}}\left(\frac{x}{L}\right)\left(\frac{L}{b}\right) \qquad \left(\frac{1}{2}\geqq\frac{x}{L}\geqq 0\right)$$

and

$$\phi=\sqrt{\frac{15}{2}}\sqrt{\epsilon_{av}-\epsilon_{cr}}\left(1-\frac{x}{L}\right)\left(\frac{L}{b}\right) \qquad \left(1\geqq\frac{x}{L}\geqq\frac{1}{2}\right)$$

A reference to figure 2 shows that the distribution of the angle ϕ is nearly linear for large rotations.

The maximum value of ϕ is $\frac{1}{2}\sqrt{\frac{15}{2}}\sqrt{\epsilon_{av}-\epsilon_{cr}}\left(\frac{L}{b}\right)$ or

$$\phi_{max}=1.37\,\frac{L}{b}\sqrt{\epsilon_{av}-\epsilon_{cr}} \qquad \text{(A40)}$$

A second approximation, which contains a small correction term to equation (A40), may be found from the relations

$$\lim_{k\to 1}\cosh^{-1}\frac{1}{\sqrt{1-k^2}}=\log\frac{2}{\sqrt{1-k^2}}$$

and

$$\lim_{k\to 1}K=\log\frac{4}{\sqrt{1-k^2}}$$

Since

$$\log\frac{2}{\sqrt{1-k^2}}=\log\frac{4}{\sqrt{1-k^2}}-\log 2$$

as $k\to 1$,

$$\cosh^{-1}\frac{1}{\sqrt{1-k^2}}=K-\log 2$$

The exact rotation at the middle of the column is given by equation (A35):

$$\phi_{max}=\sqrt{5}\,\frac{t}{b}\cosh^{-1}\frac{1}{\sqrt{1-k^2}}$$

therefore, as $k\to 1$,

$$\begin{aligned}
\phi_{max}&=\sqrt{5}\,\frac{t}{b}\,(K-\log 2)\\
&=\sqrt{5}\,\frac{t}{b}\left(\frac{mL}{\sqrt{2}\,4t}-\log 2\right)\\
&=1.37\,\frac{L}{b}\sqrt{\epsilon_{av}-\epsilon_{cr}}-1.55\,\frac{t}{b}
\end{aligned} \qquad \text{(A41)}$$

This corrective term $1.55\,\frac{t}{b}$ is always a small part of ϕ_{max}.

Variation of middle-surface strain over width of flange.—The approximate strain distribution is obtained from equation (A12) by using the approximate value of γ_b from equation (A39):

$$\epsilon_x=\epsilon_{av}+\frac{5}{4}(\epsilon_{av}-\epsilon_{cr})\left(1-3\frac{z^2}{b^2}\right) \tag{A42}$$

This result holds over most of the length of the flange but is in error near the ends and the middle where $\text{sn}\left(\frac{4Kx}{L}\right)$ has a value different from unity.

Relationship between the hinge-line, average, and critical strains.—Along the hinge line $z=0$, so that, approximately

$$(\epsilon_x)_{z=0}=\frac{9}{4}\epsilon_{av}-\frac{5}{4}\epsilon_{cr} \tag{A43}$$

Fractional shortening.—The approximate shortening is

$$e=\frac{1}{L}\int_0^L\left(\frac{9}{4}\epsilon_{av}-\frac{5}{4}\epsilon_{cr}\right)dx=\frac{9}{4}\epsilon_{av}-\frac{5}{4}\epsilon_{cr} \tag{A44}$$

and therefore is identical with ϵ_x along the hinge line $z=0$.

APPENDIX B

MAXIMUM STRENGTH OF A CRUCIFORM-SECTION COLUMN

The deformation theory of plasticity used here states that a relation exists between the stress intensity σ_i and the strain intensity e_i which is of the following form:

for loading (e_i increasing)

$$\sigma_i = E_{sec} e_i$$

for unloading (e_i decreasing)

$$d\sigma_i = E\, de_i$$

where

$$\sigma_i = \sqrt{\sigma_x^2 + \sigma_z^2 - \sigma_x\sigma_z + 3\tau^2}$$

$$e_i = \frac{2}{\sqrt{3}}\sqrt{\epsilon_x^2 + \epsilon_z^2 + \epsilon_x\epsilon_z + \frac{\gamma^2}{4}}$$

σ_x, ϵ_x stress and strain in the x-direction

σ_z, ϵ_z stress and strain in the z-direction

τ, γ shear stress and strain

In the case of a cruciform-section column compressed beyond the buckling stress σ_{cr}, the value of σ_x is the stress in the x-direction and is larger than σ_{cr} over most of the flange width. Also $\sigma_z = 0$, and with Poisson's ratio equal to 1/2, $\epsilon_z = -\frac{1}{2}\epsilon_x$; so that the fundamental stress-strain relation for increasing σ_i reduces to

$$\sqrt{\sigma_x^2 + 3\tau^2} = E_{sec}\sqrt{\epsilon_x^2 + \frac{\gamma^2}{3}}$$

in which

$$\sigma_x = E_{sec}\epsilon_x$$

$$\tau = \frac{E_{sec}}{3}\gamma$$

The value of ϵ_x at any point (x, z) of a cruciform flange is assumed from appendix A to be as in equation (A36c)

$$\epsilon_x = \frac{(t/b)^2}{2(1+\mu)} + \frac{m^2}{12} + \frac{5}{24}\frac{k^2m^2}{1+k^2}\left(1 - 3\frac{z^2}{b^2}\right)\mathrm{sn}^2\left(\frac{4Kx}{L}\right)$$

where k^2 is a parameter lying between 0 and 1 which specifies the amount of twist,

$$K = \int_0^{\pi/2} \frac{d\alpha}{\sqrt{1 - k^2\sin^2\alpha}}$$

$$m^2 = 12\left[\epsilon_{ar} - \frac{(t/b)^2}{2(1+\mu)}\right] - K^2(1+k^2)\left(\frac{4t}{L}\right)^2$$

As soon as a value is assigned to k^2 corresponding to a certain amount of twist, the quantities K and m^2 are fixed and ϵ_x may be computed.

Over most of the length of the column, $\mathrm{sn}\left(\frac{4Kx}{L}\right) \approx 1$ and, therefore, the variation of ϵ_x with x may be neglected by taking

$$\epsilon_x = \frac{(t/b)^2}{2(1+\mu)} + \frac{m^2}{12} + \frac{5}{24}\frac{k^2m^2}{1+k^2}\left(1 - 3\frac{z^2}{b^2}\right)$$

The shear strain γ arises from the twist $\frac{d\phi}{dx}$ of the flange after buckling and is proportional to the distance r away from the center line of the cross section:

$$\gamma = 2r\frac{d\phi}{dx}$$

However for insertion into the formula for strain intensity, a value of γ^2 is desired which is independent of r. Such a value may be obtained by taking the average value of γ^2 over the thickness. The mean value of γ^2 over the cross section is

$$\overline{\gamma^2} = \frac{1}{t}\int_{-t/2}^{t/2} 4r^2\left(\frac{d\phi}{dx}\right)^2 dr = \frac{t^2}{3}\left(\frac{d\phi}{dx}\right)^2 = \frac{\gamma_b^2}{3}\left(\frac{t}{b}\right)^2$$

From the theory of appendix A (equation (A31)),

$$\gamma_b=\frac{\sqrt{5}}{2}\frac{km}{\sqrt{1+k^2}}$$

over most of the section for which $\mathrm{sn}\left(\frac{4Kx}{L}\right)\approx 1$. Hence

$$\overline{\gamma^2}=\frac{5}{12}\left(\frac{t}{b}\right)^2\frac{k^2m^2}{1+k^2}$$

and thus the strain intensity $\sqrt{\epsilon_x^2+\frac{\gamma^2}{3}}$ is completely determined as soon as a value of the parameter k^2 is selected.

From the stress-strain relation the value of the stress intensity and of course E_{sec} is determined by the value of the strain intensity. (The elastic modulus E is used if the strain intensity is decreasing.) The stress σ_x may then be computed by the relation $\sigma_x=E_{sec}\epsilon_x$ as a function of the z-coordinate across the flange. The average value of σ_x across the width of the flange is then

$$\sigma_{av}=\frac{1}{b}\int_0^b \sigma_x\,dz$$

and is the average stress that would be determined from a testing machine at the value of k^2 selected.

In the actual calculations, the width b of the flange was divided into ten equal strips and the value of σ_{av} was found by a numerical summation. As the twist of the flange varies from zero to infinity, the parameter k^2 varies from zero to 1. The value of σ_{av} may be investigated as a function of k^2 and will have a maximum at some value of k^2. This maximum value of σ_{av} multiplied by the total area gives the maximum load for the cruciform flange under consideration.

REFERENCES

1. Duberg, John E., and Wilder, Thomas W., III: Column Behavior in the Plastic Stress Range. Jour. Aero. Sci., vol. 17, no. 6, June 1950, pp. 323–327.
2. Heimerl, George J.: Determination of Plate Compressive Strengths. NACA TN 1480, 1947.
3. Stowell, Elbridge Z.: A Unified Theory of Plastic Buckling of Columns and Plates. NACA Rep. 898, 1948. (Formerly NACA TN 1556.)
4. Ilyushin, A. A.: Plastichnost. OGIZ, Moskva-Leningrad, 1948, p. 115.
5. Wagner, Herbert: Torsion and Buckling of Open Sections. NACA TM 807, 1936.

U S GOVERNMENT PRINTING OFFICE: 1952